frontiers in Physics

REVIEW
published: 10 January 2022
doi: 10.3389/fphy.2021.801236

Self-Doping and the Mott-Kondo Scenario for Infinite-Layer Nickelate Superconductors

Yi-feng Yang[1,2,3]* *and Guang-Ming Zhang*[4,5]*

[1]*Beijing National Laboratory for Condensed Matter Physics and Institute of Physics, Chinese Academy of Sciences, Beijing, China,* [2]*School of Physical Sciences, University of Chinese Academy of Sciences, Beijing, China,* [3]*Songshan Lake Materials Laboratory, Dongguan, China,* [4]*State Key Laboratory of Low-Dimensional Quantum Physics and Department of Physics, Tsinghua University, Beijing, China,* [5]*Frontier Science Center for Quantum Information, Beijing, China*

We give a brief review of the Mott-Kondo scenario and its consequence in the recently-discovered infinite-layer nickelate superconductors. We argue that the parent state is a self-doped Mott insulator and propose an effective *t- J-K* model to account for its low-energy properties. At small doping, the model describes a low carrier density Kondo system with incoherent Kondo scattering at finite temperatures, in good agreement with experimental observation of the logarithmic temperature dependence of electric resistivity. Upon increasing Sr doping, the model predicts a breakdown of the Kondo effect, which provides a potential explanation of the non-Fermi liquid behavior of the electric resistivity with a power law scaling over a wide range of the temperature. Unconventional superconductivity is shown to undergo a transition from nodeless (*d+is*)-wave to nodal *d*-wave near the critical doping due to competition of the Kondo and Heisenberg superexchange interactions. The presence of different pairing symmetry may be supported by recent tunneling measurements.

Keywords: nickelate superconductor, self-doping, Mott, Kondo, t-J-K model

OPEN ACCESS

Edited by:
Danfeng Li,
City University of Hong Kong, Hong Kong SAR, China

Reviewed by:
Yusuke Nomura,
RIKEN, Japan
Liang Si,
Vienna University of Technology, Austria

***Correspondence:**
Yi-feng Yang
yifeng@iphy.ac.cn
Guang-Ming Zhang
gmzhang@tsinghua.edu.cn

Specialty section:
This article was submitted to Condensed Matter Physics, a section of the journal Frontiers in Physics

Received: *25 October 2021*
Accepted: *02 December 2021*
Published: *10 January 2022*

Citation:
Yang Y-f and Zhang G-M (2022) Self-Doping and the Mott-Kondo Scenario for Infinite-Layer Nickelate Superconductors. Front. Phys. 9:801236. doi: 10.3389/fphy.2021.801236

1 INTRODUCTION

Recent discovery of superconductivity (SC) in infinite-layer Sr-doped $NdNiO_2$ films [1] and subsequently in hole doped $LaNiO_2$ and $PrNiO_2$ films [2–5] has stimulated intensive interest in condensed matter community. Despite of many theoretical and experimental efforts, there are still debates on its electronic structures and pairing mechanism [6–21]. The study of possible Ni-based superconductivity was initially stimulated by cuprates, whose high T_c mechanism remains one of the most challenging topics in past three decades [22–25]. Many attempts have been devoted to exploring new families of high T_c superconductors. Nickelate superconductors are but one latest example of these efforts.

In undoped cuprates, Cu^{2+} ions contain nine electrons with partially occupied $3d_{x^2-y^2}$ orbitals. The oxygen $2p$ orbitals are higher in energy than the Cu $3d_{x^2-y^2}$ lower Hubbard band. Thus, cuprates belong to the so-called charge-transfer insulator. A superexchange interaction between localized Cu $3d_{x^2-y^2}$ spins is mediated by oxygen ions and causes an antiferromagnetic (AF) ground state. Upon chemical doping, holes may be introduced on the oxygen sites in the CuO_2 planes [23–25] and combine with the $3d_{x^2-y^2}$ spins to form the Zhang-Rice singlets [26], destroying the long-range AF order rapidly. In theory, these led to an effective *t-J* model, describing the holes moving on the antiferromagnetic square lattice. High temperature SC with robust *d*-wave pairing has been predicted

and established over a wide doping range [27–29]. Extending such "cuprate-Mott" conditions in other oxides has led to extensive efforts on nickel oxides [30–40]. Nickelate superconductors have a similar layered crystal structure with Ni^{1+} possessing the same $3d^9$ configuration as Cu^{2+}. As a result, theories based on Mott scenario have naturally been developed to account for nicklate superconductors.

However, there are clear evidences since the beginning suggesting that these two systems are different. Instead of a Mott insulator with AF long-range order like in cuprates, $NdNiO_2$ displays metallic behavior at high temperatures with a resistivity upturn below about 70 K, showing no sign of any magnetic long-range order in the whole measured temperature range [41]. Similar results have previously been found in $LaNiO_2$ [42]. Possible signatures of (short-range) antiferromagnetic order were reported only very recently in $Nd_{0.8}Sr_{0.2}NiO_2$ thin films by X-ray magnetic linear dichroism measurements [43] and in bulk $Nd_{0.85}Sr_{0.15}NiO_2$ by nuclear magnetic resonance (NMR) [44]. First-principles calculations have also revealed some subtle differences in their band structures. The O-2*p* orbitals are located at a deeper energy compared to that of cuprates. Nd-5*d* bands are found to hybridize with Ni-3*d* bands and produce small electron pockets in the Brillouin zone. As a consequence, holes are doped directly into Ni-3*d* orbitals rather than O-2*p* orbitals. Nickelates should thus be modelled as a self-doped Mott insulator, which implies a multi-band system with two types of charge carriers, the itinerant Nd-5*d* conduction electrons and the Ni-$3d_{x^2-y^2}$ holes, on a background lattice of Ni-$3d_{x^2-y^2}$ magnetic moments [6]. Joint analysis of the resistivity upturn and Hall coefficient at low temperatures suggests possible presence of incoherent Kondo scattering between low-density conduction electrons and localized Ni spins. A physical picture is illustrated in **Figure 1** on the square lattice. Then the basis for the Mott-Kondo scenario of nickelate superconductors has been established, leading to the proposal of an extended *t-J-K* model for a microscopic description of their low-energy properties [6, 9].

Interestingly, the Kondo hybridization does not appear significant at first glance in band structure calculations [32]. It was later realized that nickelates may host a special interstitial-*s* orbital for conduction electrons that have substantially stronger hybridization than previously thought [17]. Resonant inelastic X-ray scattering (RIXS) measurements [13, 45] confirmed the presence of hybridization between Ni $3d_{x^2-y^2}$ and Nd 5*d* orbitals. At zero temperature, the self-doping effect and the Kondo coupling produce low-energy doublon (Kondo singlet) and holon excitations on the nickel spin-1/2 background. Because of the larger charge transfer energy, nickelates were considered to have a reduced superexchange interaction between Ni^{1+} spins by almost an order of magnitude than cuprates. Raman scattering measurements seemed to confirm this expectation and estimated $J \approx 25$ meV in bulk $NdNiO_2$ [46]. However, latest RIXS measurement of magnetic excitations found a larger nearest-neighbor coupling $J_1 \approx 63.6$ meV [47] in ~10-nm-thick films, as suggested also by some recent calculations [48]. In any case, the Kondo coupling may suppress the AF long-range order and cause a phase transition to a paramagnetic metal [6]. The parent or underdoped compounds may therefore be viewed as a Kondo semimetal (KS). For large hole doping, the Ni-3*d* electrons become more itinerant and the Kondo effect breaks down, followed by an abrupt change of the charge carriers. Indeed, a sign change of the Hall coefficient has been reported in experiment [49, 50].

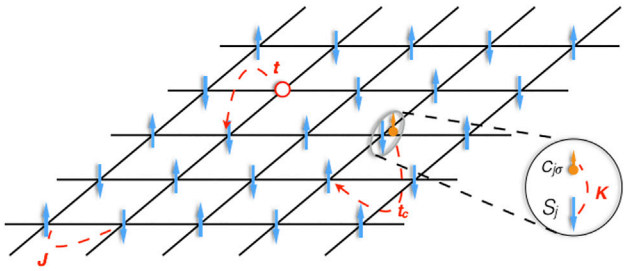

FIGURE 1 | Illustration of the self-doping and Mott-Kondo scenario for $NdNiO_2$ projected on a two-dimensional square lattice, showing one of the Ni $d_{x^2-y^2}$ electrons transferring to the Nd 5*d* orbitals. Blue arrows denote Ni-spins interacting through the Heisenberg superexchange coupling *J*. Orange arrow denotes Nd-5*d* electron, which couples to Ni-spin by the Kondo coupling *K* to form at low temperatures a Kondo singlet (doublon). Red circle represents Ni-$3d^8$ configuration, or a holon. t_c and *t* denote the hopping of doublon and holon, respectively. Figure adapted from Ref. [6]. Copyright 2020 by the American Physical Society.

The above differences have an immediate impact on candidate pairing mechanism of the superconductivity. At critical doping, the *t-J-K* model predicted possible SC transition from a gapped $(d + is)$-wave state to a gapless *d*-wave pairing state due to the competition of Kondo and superexchange interactions [9]. Latest scanning tunneling experiment (STM) also revealed two different gap structures of U and V-shapes [51], supporting the possibility of above scenario. Thus, nickelates may belong to a novel class of unconventional superconductors and one may anticipate potentially more interesting properties bridging the cuprates and heavy fermions.

In this paper, we briefly summarize the consequences of the Mott-Kondo scenario based on the extended *t-J-K* model for nickelate superconductors [6, 9]. We propose a global phase diagram upon electron and hole doping and derive a low-energy effective Hamiltonian with doublon and holon excitations in the low doping region. We then employ the renormalized mean-field theory (RMFT) to study the possibility of superconductivity and predict a phase transition of its pairing symmetry. The latter is shown to originate from the breakdown of Kondo hybridization, accompanied with non-Fermi liquid (NFL) behavior of the resistivity $\rho \sim T^{\alpha}$ near critical doping.

2 THEORY

2.1 Model Hamiltonian

To introduce the effective *t-J-K* model for describing the low-energy physics of nickelates, we start from a background lattice of Ni^{1+} $3d_{x^2-y^2}$ localized spins with a small number of self-doped holes and Nd-5 *d* conduction electrons [6]. Similar to cuprates, one expects an AF superexchange interaction between Ni^{1+} spins through the O-2*p* orbitals. This is different from heavy fermion systems, where the exchange interaction between localized spins

originates from the Ruderman-Kittel-Kasuya-Yosida (RKKY) interaction mediated by conduction electrons. It should be noted that latest RIXS measurements revealed a sizable next-nearest-neighbor coupling $J_2 \approx -10.3$ meV, implying a possible contribution from the RKKY mechanism [47]. The motion of holes on the spin lattice should be strongly renormalized as in the usual *t-J* model. There is an additional local Kondo interaction between local spins and conduction electrons. The total Hamiltonian therefore contains three terms:

$$H = H_t + H_J + H_K, \tag{1}$$

where the first term comes from the hopping of holes, the second term describes the spin lattice, and the third term gives the Kondo interaction.

For simplicity, we consider a minimal model with Ni-$3d^8$ and Nd-$5d^0$ as the vacuum. As in cuprates, the localized $3d_{x^2-y^2}$ spins on the NiO_2 plane can be described by a two-dimensional quantum Heisenberg model with nearest neighbour AF superexchange interactions,

$$H_J = J \sum_{\langle ij \rangle} S_i \cdot S_j, \tag{2}$$

whose ground state is a Mott insulator with AF long-range orders.

The self-doping effect is supported by first-principles band structure calculations [32], where the Nd 5*d* orbitals in $NdNiO_2$ are found to hybridize with the Ni 3*d* orbitals and give rise to small electron pockets in the Brillouin zone. Thus, we have a small number of Nd-5*d* conduction electrons. This is actually supported by experiment. At high temperatures, the Hall coefficient is dominated by conduction electrons giving $R_H \approx -4 \times 10^{-3}\,\mathrm{cm^3\,C^{-1}}$ for $NdNiO_2$ and $-3 \times 10^{-3}\,\mathrm{cm^3\,C^{-1}}$ for $LaNiO_2$. By contrast, in typical heavy fermion metals such as Ce*M*In_5 (*M* = Co., Rh, Ir), we have $R_H \approx -3.5 \times 10^{-4}\,\mathrm{cm^3\,C^{-1}}$ at high temperatures [52]. The larger and negative values of the Hall coefficient implies that there are only a few percent of electron-like carriers per unit cell in $NdNiO_2$ and $LaNiO_2$.

The hybridization between Ni $3d_{x^2-y^2}$ spins and conduction electrons gives the additional Kondo term:

$$H_K = -\sum_{ij\sigma}\left(t_c^{ij} c_{i\sigma}^{\dagger} c_{j\sigma} + h.c.\right) + \frac{K}{2} \sum_{j\alpha;\sigma\sigma'} S_j^{\alpha} c_{j\sigma}^{\dagger} \tau_{\sigma\sigma'}^{\alpha} c_{j\sigma'}, \tag{3}$$

where t_c^{ij} is the hopping of conduction electrons projected on the square lattice of the Ni^{1+} ions, *K* is the Kondo coupling, and τ^{α} ($\alpha = x, y, z$) are the spin-1/2 Pauli matrices. Only a single conduction band is considered for simplicity. For a low carrier density system, the average number of conduction electrons is small, i.e. $n_c = N_s^{-1} \sum_{j\sigma} \langle c_{j\sigma}^{\dagger} c_{j\sigma} \rangle \ll 1$. In reality, there may exist multiple conduction bands with three-dimensional Fermi pockets. Whether or not this can lead to other new physics requires more elaborate theoretical investigation.

The presence of magnetic impurities may be at first glance ascribed to the Nd 4*f* moments. However, the Nd^{3+} ion contains three *f* electrons forming a localized spin-3/2 moment, which acts more like a classical spin as in manganites and therefore disfavors spin-flip scattering as the quantum spin-1/2 moment. Their energy level is also far away from the Fermi energy, so it is reasonable to ignore the Nd 4*f* electrons. However, we should note that there exist different opinions on the importance of Nd-4*f* orbitals [53].

For parent compounds, self-doping also introduces an equal number of Ni $3d_{x^2-y^2}$ holes on the spin lattice. The hopping of holes on the lattice of Ni $3d_{x^2-y^2}$ spins can be described as interactions,

$$H_t = -\sum_{ij\sigma}\left(t_{ij} P_G d_{i\sigma}^{\dagger} d_{j\sigma} P_G + h.c.\right), \tag{4}$$

where $d_{i\sigma}$ and $d_{i\sigma}^{\dagger}$ are the annihilation and creation operators of the Ni $3d_{x^2-y^2}$ electrons, respectively, t_{ij} is the hopping integral between site *i* and *j*, and P_G is the Gutzwiller operator to project out doubly occupancy of local Ni $3d_{x^2-y^2}$ orbital. As in cuprates, the holes' motion is strongly renormalized due to the onsite Coulomb repulsion *U*.

Quite generally, the above effective *t-J-K* model can be replaced by the one-band Hubbard model plus a hybridization term with additional conduction electrons:

$$\begin{aligned} H = &\sum_{\mathbf{k}\sigma} E_{\mathbf{k}} d_{\mathbf{k}\sigma}^{\dagger} d_{\mathbf{k}\sigma} + U \sum_i n_{i\uparrow}^d n_{i\downarrow}^d \\ &+ \sum_{\mathbf{k}\sigma} \epsilon_{\mathbf{k}} c_{\mathbf{k}\sigma}^{\dagger} c_{\mathbf{k}\sigma} + \sum_{\mathbf{k}\sigma} V_{\mathbf{k}}\left(d_{\mathbf{k}\sigma}^{\dagger} c_{\mathbf{k}\sigma} + h.c.\right), \end{aligned} \tag{5}$$

where $E_{\mathbf{k}}$ and $\epsilon_{\mathbf{k}}$ are the dispersion of Ni $3d_{x^2-y^2}$ and conduction electrons, respectively, *U* is the onsite Coulomb interaction on Ni $3d_{x^2-y^2}$ orbital, and $V_{\mathbf{k}}$ is the hybridization. The model may also be viewed as a periodic Anderson model with dispersive *d* bands. It allows for a better treatment of charge fluctuations of the Ni $3d_{x^2-y^2}$ orbitals, in particular for large Sr doping or small Coulomb interaction. One-band model with additional electron reservoir has been studied in the literature [18–20]. More complicated models including multiple Ni-3*d* orbitals have also been proposed, focusing on different aspects of the nickelate physics such as hybridization, Hund coupling, superconductivity, and topological properties [7–17, 21]. In this work, we only consider the minimal *t-J-K* model and show that it can already capture some main features of the nickelates.

2.2 Global Phase Diagram

As is in heavy fermion systems, the *t-J-K* model contains two competing energy scales that support different ground states. The Heisenberg superexchange *J* favors an antiferromagnetic long-range order, while the Kondo coupling *K* tends to screen the local spins and form a nonmagnetic ground state. In nickelates, due to the large charge transfer energy between O-2*p* and Ni-$3d_{x^2-y^2}$ orbitals, *J* was expected to be smaller that (about 100 meV) in cuprates. First-principles calculations suggested *J* of the order of 10 meV [17], Raman scattering measurements estimated $J \approx 25$ meV in bulk $NdNiO_2$ [46], but latest RIXS experiment reported $J \approx 63.6$ meV [47]. There is at present no direct measurement of the Kondo interaction *K*. However, from the observed resistivity minimum at 70–100 K in $NdNiO_2$ and $LaNiO_2$ [1, 42], *K* may be roughly estimated to be of the order of a few hundred meV if we use the formula $T_K \approx \rho^{-1} e^{-1/K\rho}$, assume T_K to be a few Kelvin, and take a small density of states ρ of the order of 0.1 $\mathrm{eV^{-1}}$ for conduction electrons [6, 54]. This is

consistent with numerical calculations for the hybridization between Ni-3$d_{x^2-y^2}$ and interstitial *s* orbitals [17]. Thus for undoped nickelates, the Kondo coupling is a relatively large energy scale.

We may propose a global phase diagram starting from an antiferromagnetic ground state. The self-doping introduces equal numbers of conduction electrons and holes. The conduction electrons tend to form Kondo singlets with local spins due to the large *K*. Both tend to suppress the long-range AF order and causes a paramagnetic ground state. But because of the small number of conduction electrons, local spins cannot be fully Kondo screened to become delocalized. Thus, instead of a heavy fermion metal, we are actually dealing with a low carrier density Kondo system at low temperatures. Due to insufficient Kondo screening, the resistivity exhibits insulating-like behavior (upturn) because of incoherent Kondo scattering, which is typical for low carrier density Kondo systems and has been observed previously in $CeNi_{2-\delta}(As_{1-x}P_x)_2$ [55] and $NaYbSe_2$ [56].

Upon Sr (hole) doping, the number of conduction electrons may be reduced, while that of holes increases. The Kondo physics may be suppressed and replaced by the usual *t-J* model for large hole doping, resembling the physics of cuprates. On the other hand, for electron doping, we may expect to first recover the AF long-range order with reduced hole density, and then with increasing conduction electrons and Kondo screening, the AF order will be suppressed again and the system turns into a heavy fermion metal with sufficient electron doping. SC may emerge around the quantum critical point. Whether or not the AF phase may actually exist depends on how doping changes the fraction of electron and hole carriers. But in bulk $Nd_{1-x}Sr_xNiO_2$, NMR experiment has revealed short-range glassy AF ordering, supporting the possible existence of antiferromagnetism [44]. **Figure 2** summarizes possible ground states of the model on the temperature-doping plane, showing a connection between the heavy fermion and cuprate physics on two ends and the nickelates in between. However, it should be noted that current experiment on "overdoped" nickelate superconductors found a weak insulator rather than a Fermi liquid as in heavily hole-doped cuprates [50]. How exactly holes are doped in $Nd_{1-x}Sr_xNiO_2$ and whether or not multiple Ni-3*d* orbitals are needed remain an open question.

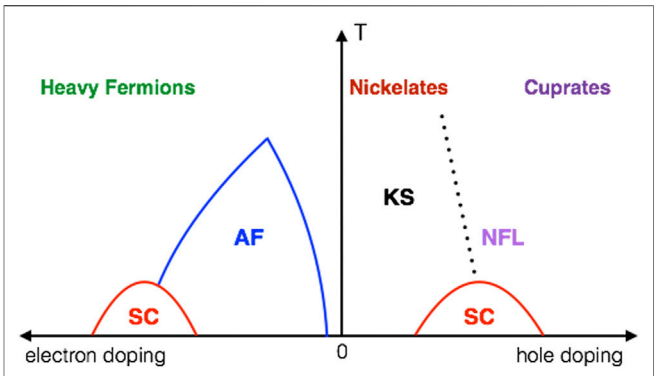

FIGURE 2 | A schematic phase diagram of the *t-J-K* model with electron and hole doping. KS stands for incoherent Kondo scattering or Kondo semimetal. Whether or not the AF phase may exist depends on details of electron and hole densities introduced by doping.

2.3 Low Energy Excitations

As shown in the phase diagram, the paramagnetic region (KS) is responsible for undoped or low doped nickelates. In this case, we have a small number (n_c) of conduction electrons per Ni-site and $n_c + p$ empty nickel sites (holons) on the NiO_2 plane, where p is the hole doping ratio. In the large *K* limit and at zero temperature, conduction electrons form Kondo singlets or doublons with local Ni spins. We may then derive an effective low-energy Hamiltonian in terms of doublons, holons, and localized spins, to describe a doped Mott metallic state with Kondo singlets [6]. A cartoon picture is given in **Figure 1**.

For this, we first introduce the pseudofermion representation for the spin-1/2 local moments:

$$S_j^+ = f_{j\uparrow}^\dagger f_{j\downarrow}, S_j^- = f_{j\downarrow}^\dagger f_{j\uparrow}, S_j^z = \frac{1}{2}\left(f_{j\uparrow}^\dagger f_{j\uparrow} - f_{j\downarrow}^\dagger f_{j\downarrow}\right),$$

where $f_{j\sigma}$ is a fermionic operator for the spinon on site *j*. The Ni $3d_{x^2-y^2}$ electron operator is given by $d_{j\sigma} = h_j^\dagger f_{j\sigma}$ with a local constraint, $h_j^\dagger h_j + \sum_\sigma f_{j\sigma}^\dagger f_{j\sigma} = 1$, if we ignore double occupancy. Here $h_j^\dagger$ is a bosonic operator creating a holon on site *j*.

The doublon operators for the on-site Kondo spin singlet and triplets may be defined as

$$b_{j0}^\dagger = \frac{1}{\sqrt{2}}\left(f_{j\uparrow}^\dagger c_{j\downarrow}^\dagger - f_{j\downarrow}^\dagger c_{j\uparrow}^\dagger\right);$$
$$b_{j1}^\dagger = f_{j\uparrow}^\dagger c_{j\uparrow}^\dagger,\ b_{j2}^\dagger = \frac{1}{\sqrt{2}}\left(f_{j\uparrow}^\dagger c_{j\downarrow}^\dagger + f_{j\downarrow}^\dagger c_{j\uparrow}^\dagger\right),\ b_{j3}^\dagger = f_{j\downarrow}^\dagger c_{j\downarrow}^\dagger.$$

The Kondo Term Then Becomes.

$$\frac{K}{2}\sum_{j\alpha;\sigma\sigma'} S_j^\alpha c_{j\sigma}^\dagger \tau_{\sigma\sigma'}^\alpha c_{j\sigma'} = \frac{K}{4}\sum_{\mu=1}^{3} b_{j\mu}^\dagger b_{j\mu} - \frac{3K}{4}\sum_j b_{j0}^\dagger b_{j0}, \quad (6)$$

which describes the doublon formation on each site, namely, the Kondo singlet or triplet pair formed by one conduction electron with a localized spinon. We see that the triplet pair costs a higher energy of *K*. Similarly, there may also exist three-particle states with one localized spinon and two conduction electrons on the same site, $e_{j\sigma}^\dagger = f_{j\sigma}^\dagger c_{j\uparrow}^\dagger c_{j\downarrow}^\dagger$, or one-particle states with one unpaired spinon only, $\tilde{f}_{j\sigma} = (1 - n_j^c) f_{j\sigma}$.

Following Refs. [57, 58], we first rewrite the Hamiltonian in terms of these new operators and then eliminate all high-energy terms containing $b_{j\mu}$ ($\mu = 1, 2, 3$) and $e_{j\sigma}$ using canonical transformation while keeping only the on-site doublon (b_{j0}) and unpaired spinons ($\tilde{f}_{j\sigma}$). This yields an effective low-energy model with a simple form

$$H_{\text{eff}} = -t\sum_{\langle ij\rangle,\sigma}\left(h_i \tilde{f}_{i\sigma}^\dagger \tilde{f}_{j\sigma} h_j^\dagger + h.c.\right) + J\sum_{\langle ij\rangle}\tilde{S}_i \cdot \tilde{S}_j$$
$$-\frac{t_c}{2}\sum_{\langle ij\rangle,\sigma}\left(b_{i0}^\dagger \tilde{f}_{i\sigma}\tilde{f}_{j\sigma}^\dagger b_{j0} + h.c.\right), \quad (7)$$

where the spin operators are $\tilde{S}_j^\alpha = \sum_{\sigma\sigma'}\tilde{f}_{j\sigma}^\dagger \frac{1}{2}\tau_{\sigma\sigma'}^\alpha \tilde{f}_{j\sigma'}$ with a local constraint $h_j^\dagger h_j + b_{j0}^\dagger b_{j0} + \sum_\sigma \tilde{f}_{j\sigma}^\dagger \tilde{f}_{j\sigma} = 1$. Here only the nearest-neighbor hopping parameters t and t_c are considered for

simplicity. For large but finite K, apart from some complicated interactions, an additional term should also be included

$$H_b = -\frac{3}{4}\left(K + \frac{t_c^2}{K}\right)\sum_j b_{j0}^\dagger b_{j0} + \frac{5t_c^2}{12K}\sum_{\langle ij\rangle} b_{i0}^\dagger b_{i0} b_{j0}^\dagger b_{j0}, \quad (8)$$

which describes the doublon condensation.

This effective Hamiltonian describes the ground state of nickelates at zero or low doping. It is similar to the usual *t-J* model for cuprates [26], but includes two types of mobile quasiparticles: doublons (Kondo singlets) and holons. It is now clear why the self-doping can efficiently suppress the AF long-range order to yield a paramagnetic ground state in nickelates. At high temperatures, doublons become deconfined, causing incoherent Kondo scattering in transport measurements. This is confirmed by the resistivity replotted in **Figure 3** as a function of temperature for both $NdNiO_2$ and $LaNiO_2$. Unlike cuprates, the resistivity exhibits metallic behavior at high temperature but shows an upturn below about 70 K. If we put the data on a linear-log scale, we find that the upturn follows exactly a logarithmic temperature ($\ln T$) dependence over a large temperature range for both compounds, which is a clear evidence for incoherent Kondo scattering typical for low carrier density Kondo systems [59]. The saturation at very low temperatures is an indication of Kondo screening. This Kondo scenario is also supported by the Hall measurement. In both compounds, the Hall coefficient R_H exhibits non-monotonic temperature dependence. It approaches a negative constant at high temperatures due to the contribution of conduction electrons, but exhibits the same $\ln T$ dependence at low temperatures. The linear relation $R_H \propto \rho$ is an indication of skew scattering by localized magnetic impurities in typical Kondo systems [60, 61].

An alternative explanation for the resistivity upturn is weak localization, where disordered holes in the NiO_2 plane may also give rise to a logarithmic correction. However, this explanation is not supported by the corresponding correction to the Hall coefficient and magnetoresistance.

2.4 Superconductivity

Experimentally, superconductivity was first observed to emerge and have an onset temperature of 14.9 K in 20% Sr doped $NdNiO_2$ thin films deposited on $SrTiO_3$ substrates [1]. From the *t-J-K* model, one may naively expect that sufficiently large doping may deplete conduction electrons and increase the number of holons, driving the system to an effective *t-J* model resembling that in cuprates. As a result, *d*-wave superconductivity may arise due to the superexchange interaction between Ni $3d_{x^2-y^2}$ electrons. However, this is not the whole truth. With increasing Sr doping, the ordinary Hall coefficient at high temperatures becomes smaller in magnitude but remains negative even in $Nd_{0.8}Sr_{0.2}NiO_2$ [1], which cannot be explained by a single carrier model but rather indicates a cancellation of electron and hole contributions. Thus, conduction electrons should still be present even at 20% Sr doping. It is thus anticipated that superconductivity in nickelates may be affected by the presence of conduction electrons and their Kondo hybridization with Ni $3d_{x^2-y^2}$ electrons.

The pairing symmetry can be studied by using the renormalized mean-field theory (RMFT) [62], which had successfully predicted the *d*-wave superconductivity in the *t-J* model for cuprates and can well describe the Fermi liquid similar to the slave-boson mean field theory. Our numerical calculations of superconductivity on the generalized *t-J-K* model have yielded a typical superconducting phase diagram in **Figure 4** [9]. The

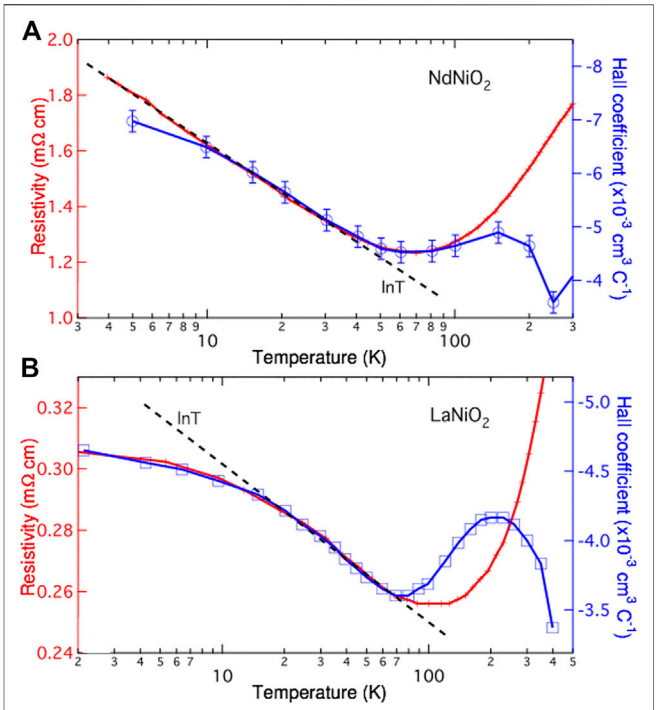

FIGURE 3 | Logarithmic scaling of the resistivity (red color) and Hall coefficient (blue color) below about 70 K for **(A)** $NdNiO_2$ with experimental data adopted from Ref. [1]; **(B)** $LaNiO_2$ reproduced from Ref. [42]. The dashed lines are the ln *T* fits. Figure adapted from Ref. [6]. Copyright 2020 by the American Physical Society.

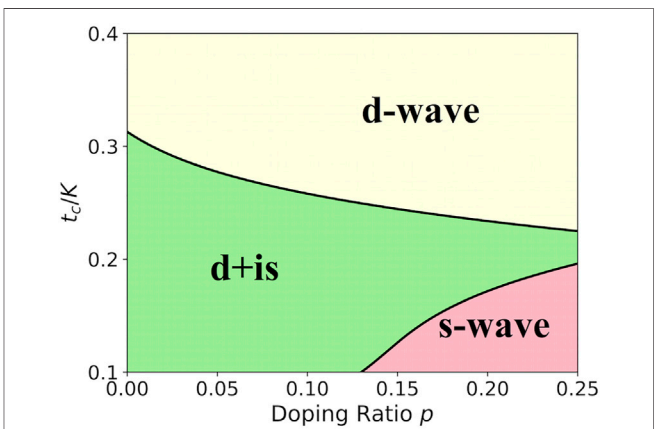

FIGURE 4 | Superconducting phase diagram of the *t-J-K* model. At small doping *p* and moderate t_c/K, the pairing symmetry is (*d* + *is*)-wave. At large t_c/K, the pairing is *d*-wave. For moderate t_c/K, the phase diagram predicts a superconducting transition from (*d* + *is*) to *d* with increasing hole doping. Figure adapted from Ref. [9]. Copyright 2020 by the American Physical Society.

pairing symmetry is found to depend on the hole concentration p and the effective strength of the Kondo hybridization controlled by the conduction electron hopping (t_c/K). For simplicity, we have taken the Kondo coupling K as the energy unit ($K = 1$), and set the AF Heisenberg spin exchange $J = 0.1$. Both the nearest-neighbor hopping $t = 0.2$ and the next-nearest-neighbor hopping $t' = -0.05$ are taken into consideration for Ni $3d$ electrons. The density of conduction electrons is taken to be $n_c = 0.1$, while their nearest-neighbor hopping t_c is chosen as a tuning parameter. Note that these parameters may in principle vary with doping in real materials. Here we fix them for simplicity in our model study and focus on the qualitative picture.

For all doping, we find a dominant d-wave pairing symmetry for large t_c/K or small K. But for low doping and moderate t_c/K, we obtain a $(d + is)$-wave pairing state that breaks the time-reversal symmetry. This is different from the conventional picture based purely on the t-J model for cuprates, where the Heisenberg superexchange interaction favors d-wave pairing [63]. The s-wave pairing should be ascribed to the Kondo coupling, which is an on-site spin exchange between localized and conduction electrons [64]. This is supported by the extended s-wave solution at large doping for small t_c/K or strong Kondo coupling. It is the combination of both effects that gives rise to the special $(d + is)$-wave superconductivity and represents a genuine feature of the nickelate superconductivity differing from cuprates or heavy fermions.

Details of RMFT calculations are explained as follows [9]. We first introduce three Gutzwiller renormalization factor to approximate the operator that projects out the doubly occupied states: $g_t = n_h/(1 + n_h)$ for the hopping t and t', $g_J = 4/(1 + n_h)^2$ for the superexchange J, and $g_K = 2/(1 + n_h)$ for the Kondo coupling K. We then define four mean-field order parameters to decouple the Heisenberg superexchange and Kondo terms:

$$\chi_{ij} = \langle d^\dagger_{i\uparrow} d_{j\uparrow} + d^\dagger_{i\downarrow} d_{j\downarrow}\rangle, \quad B = \frac{1}{\sqrt{2}}\langle d^\dagger_{j\uparrow} c^\dagger_{j\downarrow} - d^\dagger_{j\downarrow} c^\dagger_{j\uparrow}\rangle,$$
$$\Delta_{ij} = \langle d^\dagger_{i\uparrow} d^\dagger_{j\downarrow} - d^\dagger_{i\downarrow} d^\dagger_{j\uparrow}\rangle, \quad D = \frac{1}{\sqrt{2}}\langle c^\dagger_{j\uparrow} d_{j\uparrow} + c^\dagger_{j\downarrow} d_{j\downarrow}\rangle.$$

The resulting mean-field Hamiltonian has a simple bilinear form in the momentum space,

$$\mathcal{H}_{\rm mf} = \sum_{\mathbf{k}} \Psi^\dagger_{\mathbf{k}} \begin{pmatrix} \chi(\mathbf{k}) & K_D & \Delta^*(\mathbf{k}) & K_B^* \\ K_D^* & \epsilon(\mathbf{k}) & K_B^* & 0 \\ \Delta(-\mathbf{k}) & K_B & -\chi(-\mathbf{k}) & -K_D^* \\ K_B & 0 & -K_D & -\epsilon(-\mathbf{k}) \end{pmatrix} \Psi_{\mathbf{k}}, \tag{9}$$

where we have introduced the Nambu spinors $\Psi^\dagger_{\mathbf{k}} = (d^\dagger_{\mathbf{k}\uparrow}, c^\dagger_{\mathbf{k}\uparrow}, d_{-\mathbf{k}\downarrow}, c_{-\mathbf{k}\downarrow})$ and defined the matrix elements

$$\begin{aligned} \chi(\mathbf{k}) &= -\sum_\alpha \left(t g_t + \frac{3}{8} J g_J \chi_\alpha\right)\cos(\mathbf{k}\cdot\alpha) \\ &\quad -t' g_t \sum_\delta \cos(\mathbf{k}\cdot\delta) + \mu_1, \\ \epsilon(\mathbf{k}) &= -t_c \sum_\alpha \cos(\mathbf{k}\cdot\alpha) + \mu_2, \\ \Delta(\mathbf{k}) &= -\frac{3}{8} J g_J \sum_\alpha \Delta_\alpha \cos(\mathbf{k}\cdot\alpha), \\ K_D &= -\frac{3}{4} g_K K \frac{D}{\sqrt{2}}, K_B = -\frac{3}{4} g_K K \frac{B}{\sqrt{2}}. \end{aligned} \tag{10}$$

Here α denotes the vectors of the nearest-neighbor lattice sites and δ stands for those of the next-nearest-neighbor sites. μ_1 and μ_2 are chemical potentials fixing the numbers of the constrained electrons $d_{i\sigma}$ and conduction electrons $c_{i\sigma}$, respectively.

The above mean-field Hamiltonian can be diagonalized using the Bogoliubov transformation, $(d_{\mathbf{k}\uparrow}, c_{\mathbf{k}\uparrow}, d^\dagger_{-\mathbf{k}\downarrow}, c^\dagger_{-\mathbf{k}\downarrow})^T = U_{\mathbf{k}}(\alpha_{\mathbf{k}\uparrow}, \beta_{\mathbf{k}\uparrow}, \alpha^\dagger_{-\mathbf{k}\downarrow}, \beta^\dagger_{-\mathbf{k}\downarrow})^T$. The ground state is given by the vacuum of the Bogoliubov quasiparticles $\{\alpha^\dagger_{\mathbf{k}\sigma}, \beta^\dagger_{\mathbf{k}\sigma}\}$, which in turn yields the self-consistent equations for the mean-field order parameters. We will not go into more details here, but only mention that the mean-field self-consistent equations can be solved numerically and yield two dominant pairing channels of s and d-waves as shown in the phase diagram **Figure 4**. Typical results for the mean-field parameters are plotted in **Figure 5A** as a function of the doping ratio p for $t_c/K = 0.25$. For clarity, we have defined $\Delta_s = |\Delta_x + \Delta_y|/2$ and $\Delta_d = |\Delta_x - \Delta_y|/2$ to represent the respective pairing amplitudes of s and d channels. We see a clear transition from the mixed $(d + is)$-wave SC to the pure d-wave SC.

Antiferromagnetic spin fluctuations have been observed in bulk $Nd_{1-x}Sr_xNiO_2$ by NMR [44] and may also exist and play the role of pairing glues in thin films. Hence the presence of a dominant d-wave pairing at large doping is expected from the experience in cuprates. However, our results also suggest several additional features of the nickelate superconductivity that are not present in cuprates and may be examined in experiment. First, for sufficiently large Kondo coupling K, the $(d + is)$-wave SC in the low doping region breaks the time reversal symmetry and as shown in **Figure 5C** (left panel), has a nodeless gap which is distinctly different from the usual d-wave pairing with nodes along the diagonal direction. Second, we predict a quantum phase transition between this gapped $(d + is)$-wave SC to the nodal d-wave superconductivity with increasing hole doping. These features can be detected by scanning tunneling, penetration depth, or μSR experiment and serve as a support for our theory. We remark that conduction electrons play an important role in our theory of nickelate superconductivity, which is not possible in the single-band Mott picture. The importance of electron pockets is in fact supported by experimental measurements of the upper critical field [65, 66].

Recent single particle tunneling experiment [51] on superconducting nickelate thin films have also observed two distinct types of spectra: a V-shape feature with a gap maximum of 3.9 meV, a U-shape feature with a gap of about 2.35 meV, and some spectra with mixed contributions of these two components. If we attribute their different observations to different hole concentrations due to possible surface effect, the two types of spectra may correspond exactly to the two pairing states in our theory. In this sense, the scanning tunneling spectra have provided a supportive evidence for our theoretical prediction of multiple superconducting phases. Of course, the $(d + is)$-wave pairing might not exist in real materials if the Kondo coupling K is too weak or t_c/K is too large. In that case, as is seen in **Figure 4**, d-wave pairing may become dominant on the hole Fermi surface, but electron pockets may still have nodeless gap depending on their position in the Brillouin zone.

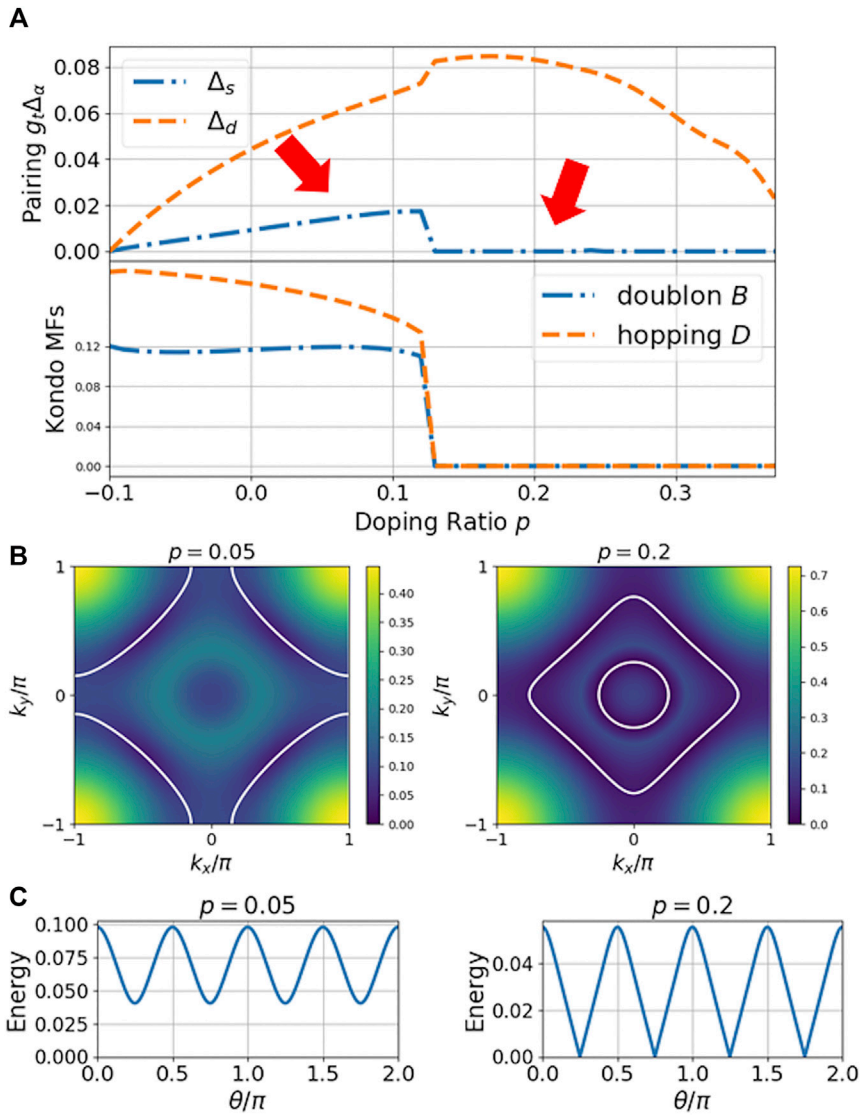

FIGURE 5 | RMFT results for $t_c/K = 0.25$. **(A)** Doping dependence of the mean-field parameters $g_t\Delta$ (upper panel) and B and D (lower panel). Comparison of **(B)** the quasiparticle excitation energy (background) and the Fermi surface (white solid line) defined as the minimal excitation energy and **(C)** superconducting gap along the Fermi surface at $p = 0.05$ ($d + is$)-wave and $p = 0.2$ (d-wave) as marked by the arrows in **(A)**. Figure adapted from Ref. [9]. Copyright 2020 by the American Physical Society.

2.5 Quantum Criticality

As shown in **Figure 5**, for moderate t_c/K, the SC transition from ($d + is$) to d-wave is accompanied with vanishing Kondo mean-field parameters B and D, which implies a breakdown of the Kondo hybridization in the large doping side. Correspondingly, the Fermi surface structures also change from a large hole-like Fermi surface around four Brillouin zone corners at low doping to two separate electron-like Fermi surfaces (from decoupled charge carriers) around the Brillouin zone center at large doping. These results may be compared with the Hall experiments in $Nd_{1-x}Sr_xNiO_2$ [49, 50], which revealed a crossover line of sign change in the temperature-doping phase diagram near the maximal T_c. The line marks a potential change in the Fermi surfaces and resembles that observed in some heavy fermion systems owing to the delocalization of localized moments [67]. It is thus attempted to link the experiment with our theoretical proposals and predict a zero-temperature quantum critical point with the SC transition and the Fermi surface change near the crossover line, although it should be cautious that they take place in different temperature region.

As a matter of fact, experiment has indeed observed quantum critical behavior in the normal state above T_c. A tentative fit of the resistivity in superconducting nickelate thin films has yielded power-law scaling with temperature, namely $\rho \sim T^\alpha$, with $\alpha = 1.1$–1.3 over a wide range [6]. **Figure 6** gives an example of the fit in $Nd_{0.8}Sr_{0.2}NiO_2$ and we obtain $\alpha \approx 1.13$ from slightly above T_c up to the room temperature. This reminds us the strange metal above T_c in optimal-doped cuprates and the non-Fermi liquid in

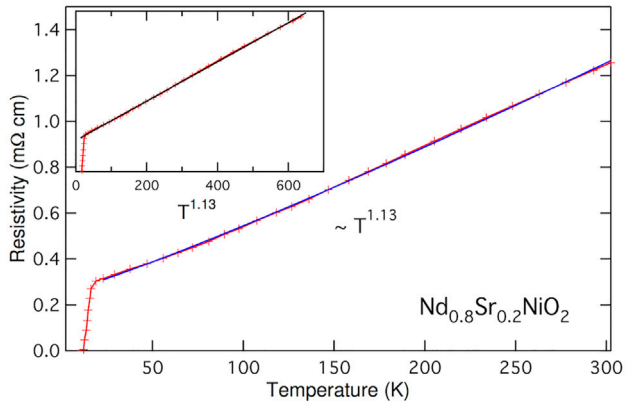

FIGURE 6 | Power-law temperature dependence of the electric resistivity above T_c = 14.9K up to the room temperature for $Nd_{0.8}Sr_{0.2}NiO_2$. The experimental data were reproduced from Ref. [1].

heavy fermion systems. Better numerical calculations are required in order to establish the exact mechanism of this scaling.

3 FUTURE PERSPECTIVE

We have introduced the picture of self-doped Mott insulator to describe the recently discovered nickelate superconductors. The self-doping effect has been generally accepted by the community and distinguishes nickelates from cuprates. We further propose a Mott-Kondo scenario and an extended *t-J-K* model based on transport measurements and electronic structure calculations. Our model bridges the usual Kondo lattice model for heavy fermions and the *t-J* model for cuprates, but shows unique features that can only be understood as an interplay of both physics. Our theory provides a natural explanation of the resistivity upturn in undoped nickelates at low temperatures, and our calculations based on the *t-J-K* model predict an exotic (d + is)-wave superconductivity that breaks the time reversal symmetry and a possible transition of the pairing symmetry at critical doping, around which the normal state exhibits non-Fermi liquid behavior above T_c. This implies that nickelate superconductors are a novel class of unconventional superconductors. Thus, exploration of new physics based on our theory will be an interesting direction for future investigations.

Currently there still exist different opinions on the effect of Sr doping. Some argued that holes may occupy other Ni 3*d* orbitals and the Hund coupling may favor a high spin state (S = 1) [8, 14, 16]. This scenario seems inconsistent with joint analyses of XAS and RIXS experiments [18] and a number of other calculations [11, 20]. Nevertheless, our model allows for a straightforward multi-orbital extension by considering a two-band Hubbard model of Ni 3*d* orbitals (or its projection at large U) plus hybridization with additional conduction bands. So far, bulk nickelates have not been found superconductive and many issues remain to be answered both in theory and in experiment [68]. Our proposal of the self-doping effect, the Mott-Kondo scenario, and the *t-J-K* model provides a promising starting basis for future investigations.

AUTHOR CONTRIBUTIONS

All authors listed have made a substantial, direct, and intellectual contribution to the work and approved it for publication.

FUNDING

This work was supported by the National Natural Science Foundation of China (Nos. 11774401, 11974397, and 12174429), the National Key Research and Development Program of MOST of China (Nos. 2017YFA0303103 and 2017YFA0302902), and the Strategic Priority Research Program of CAS (Grand No. XDB33010100).

REFERENCES

1. Li D, Lee K, Wang BY, Osada M, Crossley S, Lee HR, et al. Superconductivity in an Infinite-Layer Nickelate. *Nature* (2019) 572:624–7. doi:10.1038/s41586-019-1496-5
2. Osada M, Wang BY, Goodge BH, Lee K, Yoon H, Sakuma K, et al. A Superconducting Praseodymium Nickelate with Infinite Layer Structure. *Nano Lett* (2020) 20:5735–40. doi:10.1021/acs.nanolett.0c01392
3. Osada M, Wang BY, Lee K, Li D, Hwang HY. Phase Diagram of Infinite Layer Praseodymium Nickelate $Pr_{1-x}Sr_xNiO_2$ Thin Films. *Phys Rev Mater* (2020) 4: 121801. doi:10.1103/physrevmaterials.4.121801
4. Zeng S, Li C, Chow L, Cao Y, Zhang Z, Tang C, et al. Superconductivity in Infinite-Layer Lanthanide Nickelates. arXiv preprint arXiv:2105.13492 (2021).
5. Osada M, Wang BY, Goodge BH, Harvey SP, Lee K, Li D, et al. Nickelate Superconductivity without Rare-Earth Magnetism: (La, Sr)NiO_2. arXiv preprint arXiv:2105.13494 (2021).
6. Zhang G-M, Yang Y-f., Zhang F-C. Self-doped mott Insulator for Parent Compounds of Nickelate Superconductors. *Phys Rev B* (2020) 101(R):020501. doi:10.1103/PhysRevB.101.020501
7. Nomura Y, Hirayama M, Tadano T, Yoshimoto Y, Nakamura K, Arita R. Formation of a Two-Dimensional Single-Component Correlated Electron System and Band Engineering in the Nickelate Superconductor $NdNiO_2$. *Phys Rev B* (2019) 100:205138. doi:10.1103/PhysRevB.100.205138
8. Hu L-H, Wu C. Two-band Model for Magnetism and Superconductivity in Nickelates. *Phys Rev Res* (2019) 1:032046. doi:10.1103/PhysRevResearch.1.032046
9. Wang Z, Zhang G-M, Yang Y-f., Zhang F-C. Distinct Pairing Symmetries of Superconductivity in Infinite-Layer Nickelates. *Phys Rev B* (2020) 102(R): 220501. doi:10.1103/PhysRevB.102.220501
10. Botana AS, Norman MR. Similarities and Differences between $LaNiO_2$ and $CaCuO_2$ and Implications for Superconductivity. *Phys Rev X* (2020) 10:011024. doi:10.1103/PhysRevX.10.011024
11. Jiang M, Berciu M, Sawatzky GA. Critical Nature of the Ni Spin State in Doped $NdNiO_2$. *Phys Rev Lett* (2020) 124:207004. doi:10.1103/PhysRevLett.124.207004
12. Sakakibara H, Usui H, Suzuki K, Kotani T, Aoki H, Kuroki K. Model Construction and a Possibility of Cupratelike Pairing in a New d^9 Nickelate Superconductor (Nd,Sr)NiO_2. *Phys Rev Lett* (2020) 125:077003. doi:10.1103/PhysRevLett.125.077003

13. Hepting M, Li D, Jia CJ, Lu H, Paris E, Tseng Y, et al. Electronic Structure of the Parent Compound of Superconducting Infinite-Layer Nickelates. *Nat Mater* (2020) 19:381–5. doi:10.1038/s41563-020-0761-110.1038/s41563-019-0585-z
14. Zhang Y-H, Vishwanath A. Type-II t–J Model in Superconducting Nickelate $Nd_{1-x}Sr_xNiO_2$. *Phys Rev Res* (2020) 2:023112. doi:10.1103/PhysRevResearch.2.023112
15. Lechermann F. Multiorbital Processes Rule the $Nd_{1-x}Sr_xNiO_2$ Normal State. *Phys Rev X* (2020) 10:041002. doi:10.1103/PhysRevX.10.041002
16. Werner P, Hoshino S. Nickelate Superconductors: Multiorbital Nature and Spin Freezing. *Phys Rev B* (2019) 101:041104. doi:10.1103/PhysRevB.101.041104
17. Gu Y, Zhu S, Wang X, Hu J, Chen H. A Substantial Hybridization between Correlated Ni-D Orbital and Itinerant Electrons in Infinite-Layer Nickelates. *Commun Phys* (2020) 3:1–9. doi:10.1038/s42005-020-0347-x
18. Rossi M, Lu H, Nag A, Li D, Osada M, Lee K, et al. Orbital and Spin Character of Doped Carriers in Infinite-Layer Nickelates. arXiv preprint arXiv:2011.00595 (2020).
19. Kitatani M, Si L, Janson O, Arita R, Zhong Z, Held K. Nickelate Superconductors-A Renaissance of the One-Band Hubbard Model. *npj Quan Mater.* (2020) 5:59. doi:10.1038/s41535-020-00260-y
20. Higashi K, Winder M, Kuneš J, Hariki A. Core-Level X-Ray Spectroscopy of Infinite-Layer Nickelate: LDA+DMFT Study. *Phys Rev X* (2021) 11:041009. doi:10.1103/PhysRevX.11.041009
21. Gao J, Peng S, Wang Z, Fang C, Weng H. Electronic Structures and Topological Properties in Nickelates $Ln_{n+1}Ni_nO_{2n+2}$. *Natl Sci Rev* (2021) 8:nwaa218. doi:10.1093/nsr/nwaa218
22. Bednorz JG, Müller KA. Possible highT C Superconductivity in the Ba-La-Cu-O System. *Z Physik B - Condensed Matter* (1986) 64:189–93. doi:10.1007/BF01303701
23. Anderson PW. The Resonating Valence Bond State in La_2CuO_4 and Superconductivity. *Science* (1987) 235:1196–8. doi:10.1126/science.235.4793.1196
24. Anderson PW, Lee PA, Randeria M, Rice TM, Trivedi N, Zhang FC. The Physics behind High-Temperature Superconducting Cuprates: the plain Vanilla Version of RVB. *J Phys Condens Matter* (2004) 16:R755–R769. doi:10.1088/0953-8984/16/24/r02
25. Lee PA, Nagaosa N, Wen X-G. Doping a Mott Insulator: Physics of High-Temperature Superconductivity. *Rev Mod Phys* (2006) 78:17–85. doi:10.1103/RevModPhys.78.17
26. Zhang FC, Rice TM. Effective Hamiltonian for the Superconducting Cu Oxides. *Phys Rev B* (1988) 37:3759–61. doi:10.1103/PhysRevB.37.3759
27. Shen Z-X, Dessau DS, Wells BO, King DM, Spicer WE, Arko AJ, et al. Anomalously Large gap Anisotropy in the a-b Plane of $Bi_2Sr_2CaCu_2O_{8+\delta}$. *Phys Rev Lett* (1993) 70:1553–6. doi:10.1103/physrevlett.70.1553
28. Wollman DA, Van Harlingen DJ, Lee WC, Ginsberg DM, Leggett AJ. Experimental Determination of the Superconducting Pairing State in YBCO from the Phase Coherence of YBCO-Pb dc SQUIDs. *Phys Rev Lett* (1993) 71:2134–7. doi:10.1103/PhysRevLett.71.2134
29. Tsuei CC, Kirtley JR, Chi CC, Yu-Jahnes LS, Gupta A, Shaw T, et al. Pairing Symmetry and Flux Quantization in a Tricrystal Superconducting Ring of $YBa_2Cu_3O_{7-\delta}$. *Phys Rev Lett* (1994) 73:593–6. doi:10.1103/physrevlett.73.593
30. Anisimov VI, Bukhvalov D, Rice TM. Electronic Structure of Possible Nickelate Analogs to the Cuprates. *Phys Rev B* (1999) 59:7901–6. doi:10.1103/PhysRevB.59.7901
31. Hayward MA, Green MA, Rosseinsky MJ, Sloan J. Sodium Hydride as a Powerful Reducing Agent for Topotactic Oxide Deintercalation: Synthesis and Characterization of the Nickel(I) Oxide $LaNiO_2$. *J Am Chem Soc* (1999) 121:8843–54. doi:10.1021/ja991573i
32. Lee K-W, Pickett WE. Infinite-layer $LaNiO_2$: Ni^{1+} is not Cu^{2+}. *Phys Rev B* (2004) 70:165109. doi:10.1103/PhysRevB.70.165109
33. Botana AS, Pardo V, Norman MR. Electron Doped Layered Nickelates: Spanning the Phase Diagram of the Cuprates. *Phys Rev Mater* (2017) 1:021801. doi:10.1103/PhysRevMaterials.1.021801
34. Chaloupka J, Khaliullin G. Orbital Order and Possible Superconductivity in $LaNiO_3/LaMO_3$ Superlattices. *Phys Rev Lett* (2008) 100:016404. doi:10.1103/PhysRevLett.100.016404
35. Hansmann P, Yang X, Toschi A, Khaliullin G, Andersen OK, Held K. Turning a Nickelate Fermi Surface into a Cupratelike One through Heterostructuring. *Phys Rev Lett* (2009) 103:016401. doi:10.1103/PhysRevLett.103.016401
36. Middey S, Chakhalian J, Mahadevan P, Freeland JW, Millis AJ, Sarma DD. Physics of Ultrathin Films and Heterostructures of Rare-Earth Nickelates. *Annu Rev Mater Res* (2016) 46:305–34. doi:10.1146/annurev-matsci-070115-032057
37. Boris AV, Matiks Y, Benckiser E, Frano A, Popovich P, Hinkov V, et al. Dimensionality Control of Electronic Phase Transitions in Nickel-Oxide Superlattices. *Science* (2011) 332:937–40. doi:10.1126/science.1202647
38. Benckiser E, Haverkort MW, Brück S, Goering E, Macke S, Frañó A, et al. Orbital Reflectometry of Oxide Heterostructures. *Nat Mater* (2011) 10:189–93. doi:10.1038/nmat2958
39. Disa AS, Kumah DP, Malashevich A, Chen H, Arena DA, Specht ED, et al. Orbital Engineering in Symmetry-Breaking Polar Heterostructures. *Phys Rev Lett* (2015) 114:026801. doi:10.1103/PhysRevLett.114.026801
40. Zhang J, Botana AS, Freeland JW, Phelan D, Zheng H, Pardo V, et al. Large Orbital Polarization in a Metallic Square-Planar Nickelate. *Nat Phys* (2017) 13:864–9. doi:10.1038/nphys4149
41. Hayward MA, Rosseinsky MJ. Synthesis of the Infinite Layer Ni(I) Phase $NdNiO_{2+x}$ by Low Temperature Reduction of $NdNiO_3$ with Sodium Hydride. *Solid State Sci* (2003) 5:839–50. doi:10.1016/S1293-2558(03)00111-0
42. Ikeda A, Krockenberger Y, Irie H, Naito M, Yamamoto H. Direct Observation of Infinite NiO_2 Planes in $LaNiO_2$ Films. *Appl Phys Express* (2016) 9:061101. doi:10.7567/APEX.9.061101
43. Zhou X, Zhang X, Yi J, Qin P, Feng Z, Jiang P, et al. Antiferromagnetism in Ni-Based Superconductors. arXiv preprint arXiv:2110.14915 (2021).
44. Cui Y, Li C, Li Q, Zhu X, Hu Z, Yang Y-f., et al. NMR Evidence of Antiferromagnetic Spin Fluctuations in $Nd_{0.85}Sr_{0.15}NiO_2$. *Chin Phys. Lett.* (2021) 38:067401. doi:10.1088/0256-307X/38/6/067401
45. Goodge BH, Li D, Lee K, Osada M, Wang BY, Sawatzky GA, et al. Doping Evolution of the Mott-Hubbard Landscape in Infinite-Layer Nickelates. *Proc Natl Acad Sci USA* (2021) 118:e2007683118. doi:10.1073/pnas.2007683118
46. Fu Y, Wang L, Cheng H, Pei S, Zhou X, Chen J, et al. Core-level X-ray Photoemission and Raman Spectroscopy Studies on Electronic Structures in Mott-Hubbard Type Nickelate Oxide $NdNiO_2$. arXiv preprint arXiv:1911.03177 (2019).
47. Lu H, Rossi M, Nag A, Osada M, Li DF, Lee K, et al. Magnetic Excitations in Infinite-Layer Nickelates. *Science* (2021) 373:213–6. doi:10.1126/science.abd7726
48. Been E, Lee WS, Hwang HY, Cui Y, Zaanen J, Devereaux T, et al. Electronic Structure Trends across the Rare-Earth Series in Superconducting Infinite-Layer Nickelates. *Phys Rev X* (2021) 11:011050. doi:10.1103/physrevx.11.011050
49. Li D, Wang BY, Lee K, Harvey SP, Osada M, Goodge BH, et al. Superconducting Dome in $Nd_{1-x}Sr_xNiO_2$ Infinite Layer Films. *Phys Rev Lett* (2020) 125:027001. doi:10.1103/PhysRevLett.125.027001
50. Zeng S, Tang CS, Yin X, Li C, Li M, Huang Z, et al. Phase Diagram and Superconducting Dome of Infinite-Layer $Nd_{1-x}Sr_xNiO_2$ Thin Films. *Phys Rev Lett* (2020) 125:147003. doi:10.1103/PhysRevLett.125.147003
51. Gu Q, Li Y, Wan S, Li H, Guo W, Yang H, et al. Single Particle Tunneling Spectrum of Superconducting $Nd_{1-x}Sr_xNiO_2$ Thin Films. *Nat Commun* (2020) 11:1–7. doi:10.1038/s41467-020-19908-1
52. Hundley M, Malinowski A, Pagliuso P, Sarrao J, Thompson J. Anomalous F-Electron Hall Effect in the Heavy-Fermion System $CeTIn_5$ (T=Co, Ir, or Rh). *Phys Rev B* (2004) 70:035113. doi:10.1103/physrevb.70.035113
53. Jiang P, Si L, Liao Z, Zhong Z. Electronic Structure of Rare-Earth Infinite-Layer $RNiO_2$(R=La,Nd). *Phys Rev B* (2019) 100:201106. doi:10.1103/PhysRevB.100.201106
54. Yang Y-f., Fisk Z, Lee H-O, Thompson JD, Pines D. Scaling the Kondo Lattice. *Nature* (2008) 454:611–3. doi:10.1038/nature07157
55. Chen J, Wang Z, Li Y, Feng C, Dai J, Xu Za., et al. Heavy Fermion Quantum Criticality at Dilute Carrier Limit in $CeNi_{2-\delta}(As_{1-x}P_x)_2$. *Sci Rep* (2019) 9:1–10. doi:10.1038/s41598-019-48662-8
56. Xu Y, Sheng Y, Yang YF. Mechanism of the Insulator-To-Metal Transition and Superconductivity in the Spin Liquid Candidate $NaYbSe_2$ under Pressure. arXiv preprint arXiv:2108.03218 (2021).

57. Lacroix C. Some Exact Results for the Kondo Lattice with Infinite Exchange Interaction. *Solid State Commun* (1985) 54:991–4. doi:10.1016/0038-1098(85)90171-1
58. Sigrist M, Ueda K, Tsunetsugu H. Ferromagnetism of the Kondo Lattice in the Low-Carrier-Concentration Limit. *Phys Rev B* (1992) 46:175–83. doi:10.1103/PhysRevB.46.175
59. Hewson AC. *The Kondo Problem to Heavy Fermions*. Cambridge: Cambridge University Press (1993).
60. Fert A, Levy PM. Theory of the Hall Effect in Heavy-Fermion Compounds. *Phys Rev B* (1987) 36:1907–16. doi:10.1103/physrevb.36.1907
61. Nagaosa N, Sinova J, Onoda S, MacDonald AH, Ong NP. Anomalous Hall Effect. *Rev Mod Phys* (2010) 82:1539–92. doi:10.1103/RevModPhys.82.1539
62. Zhang FC, Gros C, Rice TM, Shiba H. A Renormalised Hamiltonian Approach to a Resonant Valence Bond Wavefunction. *Supercond Sci Technol* (1988) 1:36–46. doi:10.1088/0953-2048/1/1/009
63. Wu X, Di Sante D, Schwemmer T, Hanke W, Hwang HY, Raghu S, Thomale R. Robust $d_{x^2-y^2}$-wave Superconductivity of Infinite-Layer Nickelates-Wave Superconductivity of Infinite-Layer Nickelates. *Phys Rev B* (2020) 101:060504. doi:10.1103/PhysRevB.101.060504
64. Bodensiek O, Žitko R, Vojta M, Jarrell M, Pruschke T. Unconventional Superconductivity from Local Spin Fluctuations in the Kondo Lattice. *Phys Rev Lett* (2013) 110:146406. doi:10.1103/PhysRevLett.110.146406
65. Xiang Y, Li Q, Li Y, Yang H, Nie Y, Wen H-H. Physical Properties Revealed by Transport Measurements for Superconducting $Nd_{0.8}Sr_{0.2}NiO_2$ Thin Films. *Chin Phys. Lett.* (2021) 38:047401. doi:10.1088/0256-307X/38/4/047401
66. Wang BY, Li D, Goodge BH, Lee K, Osada M, Harvey SP, et al. Isotropic Pauli-Limited Superconductivity in the Infinite-Layer Nickelate $Nd_{0.775}Sr_{0.225}NiO_2$. *Nat Phys* (2021) 17:473–7. doi:10.1038/s41567-020-01128-5
67. Yang Y-f., Pines D, Lonzarich G. Quantum Critical Scaling and Fluctuations in Kondo Lattice Materials. *Proc Natl Acad Sci USA* (2017) 114:6250–5. doi:10.1073/pnas.1703172114
68. Gu Q, Wen HH. Superconductivity in Nickel Based 112 Systems. arXiv preprint arXiv:2109.07654 (2021).

Conflict of Interest: The authors declare that the research was conducted in the absence of any commercial or financial relationships that could be construed as a potential conflict of interest.

Publisher's Note: All claims expressed in this article are solely those of the authors and do not necessarily represent those of their affiliated organizations, or those of the publisher, the editors and the reviewers. Any product that may be evaluated in this article, or claim that may be made by its manufacturer, is not guaranteed or endorsed by the publisher.